An Analytic Analysis of a Traveling-wave Stark Decelerator

Bachelor Research Project

Bart Schellenberg

Supervisor:
Steven Hoekstra

Second Examiner:
Ronnie Hoekstra

July 3, 2020

A traveling-wave Stark decelerator makes use of inhomogeneous electric fields to decelerate neutral polar molecules. So far, mostly numerical results exist on the fields and behaviour of particles inside the decelerator. However, since these results are numerically generated using simulations, a full understanding of the results may be overlooked. In order to expand the understanding of and improve simulations on the mechanics of the setup, some analytic models are studied. These models include a function for the electric and effective fields as well as a one-dimensional analysis on the phasespace stability of molecules. Under a few approximations, the one-dimensional equation of motion is shown to be isomorphic to that of a biased pendulum.

Contents

1 Introduction **3**

2 Working Principles **4**
2.1 Traveling-wave Stark Decelerator 4
2.2 Standing-wave Stark Decelerator 5

3 Beam Environment **6**
3.1 Single Ring Field 6
3.2 Ring Array Field 8
3.3 Central Axis Field 10
3.4 Analytic Field 13

4 Effective Field **16**
4.1 Stark Effect - Classical View 16
4.2 Stark Effect - Quantum Mechanical View 17
4.3 Particle Waterslide 18
4.3.1 Static Polarization 18
4.3.2 Linear Polarization 19
4.3.3 BaF Field 19

5 One-Dimensional Motion **21**
5.1 Equation of Motion 21
5.1.1 Phase Position 21
5.1.2 First Harmonic 22
5.2 Biased Pendulum 22
5.2.1 Isomorphism of the Equation of Motion 23
5.2.2 Alternative Orientations 24
5.3 Phase Stability 25
5.3.1 Equilibrium States 25
5.3.2 One-Dimensional Traps 26
5.3.3 Phasespace Trajectories 27

6 Conclusion **30**
6.1 Outlook 30

7 Appendix **33**
7.1 Multivariable Taylor Expansion 33
7.2 Degenerate Perturbation Theory 35

1 Introduction

The Stark effect describes the perturbation of atomic and molecular energy levels due to an external electric field. Much like the Zeeman effect for magnetic fields, the Stark effect causes energy levels to shift and degenerate levels to split. By making use of an inhomogeneous electric field, an effective force can be exerted on a particle. A Stark decelerator exploits this feature in order to decelerate polar molecules as to decrease their (directional) temperature.

Interest for cold molecules is found in many areas of research such as quantum computation[11], collision dynamics[4], high-resolution spectroscopy[2] or measurements on the permanent electric dipole moment of an electron[1].

The aim of this project is to look into analytic models that can be used to describe the fields and the behaviour/stability of molecules in a Stark decelerator. In particular, the traveling-wave Stark decelerator described in section 2.1. Where necessary, the analyses will be supplemented by numerically generated graphics and solutions. Building a better model for the fields and the stability of particles greatly helps in understanding their behaviour as well as to optimize and improve numerical simulations.

The report will begin to consider the working principles and constraints of a Stark decelerator in section 2. Following are two examples of a Stark decelerator in sections 2.1 and 2.2, the first of which has been at the center of this project. Both examples have had a significant contribution to the results presented in this report. In section 3 a fully analytical description of the electric field inside the traveling-wave decelerator is derived. Using a simplified notation for the Stark energy, the effective fields and forces as experienced by particles is discussed in section 4. Once the effective fields are obtained, the equation of motion and stability is analyzed for particles confined to the central axis of the decelerator in section 5. This is the so-called one-dimensional case. The behaviour is explained through the isomorphism of the equation of motion and that of a biased pendulum.

2 Working Principles

A Stark decelerator can be used to control the longitudinal velocity of a particle beam. Results are obtained by creating a spatially oscillating electric potential that forms local minima in the electric field strength. These local minima function as traps for particles in a low field seeking (LFS) state. By decreasing (or increasing) the oscillation frequency of the field, particles can be made to decelerate (or accelerate).

Following Earnshaw's theorem an electrostatic field cannot obtain a local maximum. This has the consequence that similar traps for high field seeking (HFS) states do not exist. As a result, HFS states in a Stark decelerator are highly unstable. Therefore, mainly LFS states will be considered, unless specified otherwise.

2.1 Traveling-wave Stark Decelerator

The decelerator at the center of this project is the traveling-wave decelerator in Groningen[9]. In the traveling-wave decelerator a large series of circular electrodes is used. Every eighth electrode is electrically connected and hence will carry the same charge. By tuning the charge on the electrodes, three-dimensional electrostatic traps are formed. By including a temporal dependence of the charge, these traps are made to move at a desired speed along the decelerator. A schematic of the setup is shown in figure 1. In figure 2 a contour

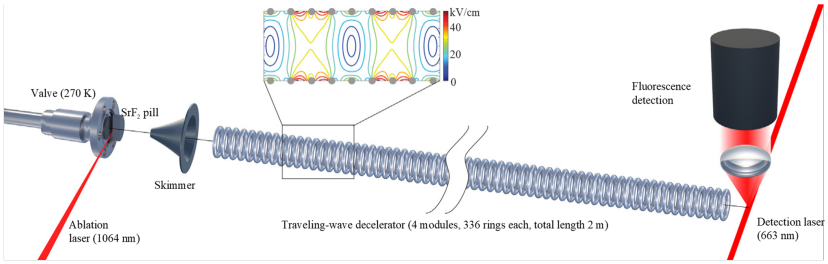

Figure 1: *Schematic of a traveling-wave Stark decelerator[10]. (Please note that the figure is slightly outdated and additional modules have been added up to a length of* $4.5m$*.)*

and density plot of the electric field strength inside the decelerator is shown. The figure shows a snapshot for one moment in time. A further analysis of the behaviour of the field is given in section 3 and in particular sections 3.2 and 3.4. An overview of the technical details relevant to this report is given in table 1.

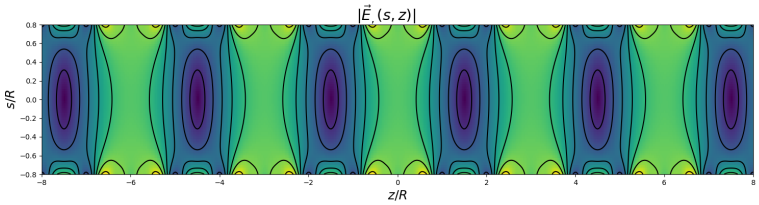

Figure 2: *Three dimensional traps in a traveling-wave decelerator. The cylindrical invariance of the system allows for a two-dimensional plot. Here, s denotes the radial distance, z the position on the central-axis and R the radius of the circular electrodes.*

Description	**Symbol**	**Value**
ring radius	R	2 mm
ring interval	d	1.5 mm
charge amplitude	V_0	$\sim 1 - 10$ kV
modulation function	a_τ	$\sin(\frac{\tau\pi}{4} - \omega(t)t + \delta)$

Table 1: *Some configuration of the traveling-wave Stark decelerator[18]. The variables given were used in producing the graphics of this report. The modulation function determines the relative charge on each ring, with $\tau \in [0, 7]$ (see section 3.2).*

2.2 Standing-wave Stark Decelerator

Another example of a Stark decelerator is the standing-wave decelerator used in Berlin[3]. This decelerator makes use of a long series of stages where every other stage is electrically connected. Each stage consists of two metal rods place suspended on both sides of the beam axis. By charging and grounding the rods alternately, the electric field is switched between two configurations. This has the effect of creating a standing wave along the beam trajectory. A schematic of the setup is shown in figure 3. Through a Fourier series expansion, the field is described as a series of traveling waves. According to [8], the motion of a particle is then almost solely determined by the by the wave traveling with the average velocity of the particle.

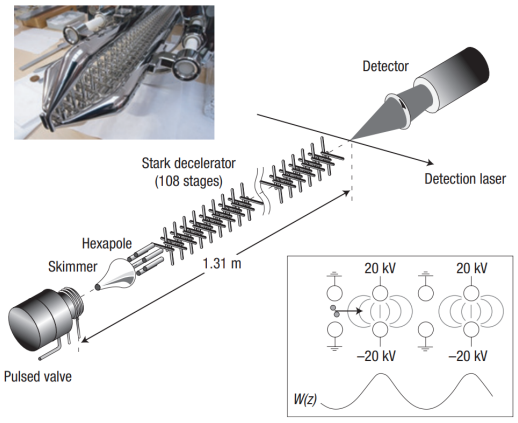

Figure 3: *Schematic of a standing-wave Stark decelerator[16].*

3 Beam Environment

Before one can begin to describe the behaviour of particles in the field of a Stark decelerator, it is first necessary to find an expression for the field itself. The superposition of the electric potential[6] allows for the total field to be described by the addition of the contributions of each electrode individually. The aim of this section is to find an expression for the electric field in a building-up manner.

3.1 Single Ring Field

The smallest sub-components of the decelerator consist of the small circular electrodes. In general, the electric potential due to some arbitrary distribution of charge is obtained by

$$V(\vec{r}) = \frac{1}{4\pi\epsilon_0} \int \frac{\rho(\vec{r}')}{|\vec{r} - \vec{r}'|} d^3r',$$

where $\rho(\vec{r}')$ denotes the charge density distribution function. Given the cylindrical symmetry of the electrodes, it is more convenient to work with cylindrical coordinates. That is, $d^3r' \to Rd\varphi'$, with R the (fixed) radius of one ring and $\vec{r} = \vec{0}$ at the center of the ring. Then

$$V(\vec{r}) = \frac{1}{4\pi\epsilon_0} \int_0^{2\pi} \frac{\rho(\vec{r}')}{|\vec{r} - \vec{r}'|} Rd\varphi'.$$

Assuming a uniform charge distribution on the ring, the charge density can be pulled through the integral to get

$$V(\vec{r}) = \frac{\rho}{4\pi\epsilon_0} \int_0^{2\pi} \frac{1}{|\vec{r} - \vec{r}'|} d\varphi'.$$

Before continuing, it is good to first rewrite the integrand into a more feasible form. Using the cylindrical coordinates s for radial distance, z for the position along the central axis and φ for the angular direction. The ring is then fully positioned in the xy-plane, such that $z' = 0$.

$$\begin{aligned}
|\vec{r} - \vec{r}'| &= \sqrt{(x - x')^2 + (y - y')^2 + (z - 0)^2}, \\
&= \sqrt{(s\cos\varphi - R\cos\varphi')^2 + (s\sin\varphi - R\sin\varphi')^2 + z^2}, \\
&= \sqrt{s^2 + R^2 + z^2 - 2sR(\cos\varphi\cos\varphi' + \sin\varphi\sin\varphi')}, \\
&= \sqrt{s^2 + R^2 + z^2 - 2sR\cos(\varphi - \varphi')}.
\end{aligned}$$

Substituting this back into the integral gives

$$V(s, \varphi, z) = \frac{\rho}{4\pi\epsilon_0} \int_0^{2\pi} \frac{1}{\sqrt{s^2 + R^2 + z^2 - 2sR\cos(\varphi - \varphi')}} d\varphi'.$$

By exploiting the identity that the cosine function is an even function, one can half the integral size to

$$V(s, \varphi, z) = \frac{\rho}{2\pi\epsilon_0} \int_{\varphi}^{\varphi+\pi} \frac{1}{\sqrt{s^2 + R^2 + z^2 - 2sR\cos(\varphi - \varphi')}} d\varphi'.$$

To finish, by making use of the cylindrical invariance of the system under rotations φ, the field due to a single ring becomes

$$V_{\mathcal{R}}(s, z) = \frac{\rho}{2\pi\epsilon_0} \int_0^{\pi} \frac{1}{\sqrt{R^2 + s^2 + z^2 - 2sR\cos\varphi}} d\varphi, \tag{1}$$

where the original φ' has now been replaced by the symbol φ. To make clear that equation (1) refers to the field following a single ring, the subscript $\mathcal{R}$ will be included from now on.

The electric field is then obtained by taking the negative gradient of the potential $\vec{E} = -\vec{\nabla} V_{\mathcal{R}}$, with $\vec{\nabla} V = \partial_s V \hat{s} + \frac{1}{s}\partial_\phi V \hat{\phi} + \partial_z V \hat{z}$ the gradient in cylindrical coordinates. Then

$$\vec{E}_{\mathcal{R}} = -\frac{\rho}{2\pi\epsilon_0} \int_0^{\pi} \frac{(s - R\cos\varphi)\hat{s} + z\hat{z}}{(R^2 + s^2 + z^2 - 2sR\cos\varphi)^{3/2}} d\varphi. \tag{2}$$

An overview of the graphs following equations (1) and (2) is given in figure 4.

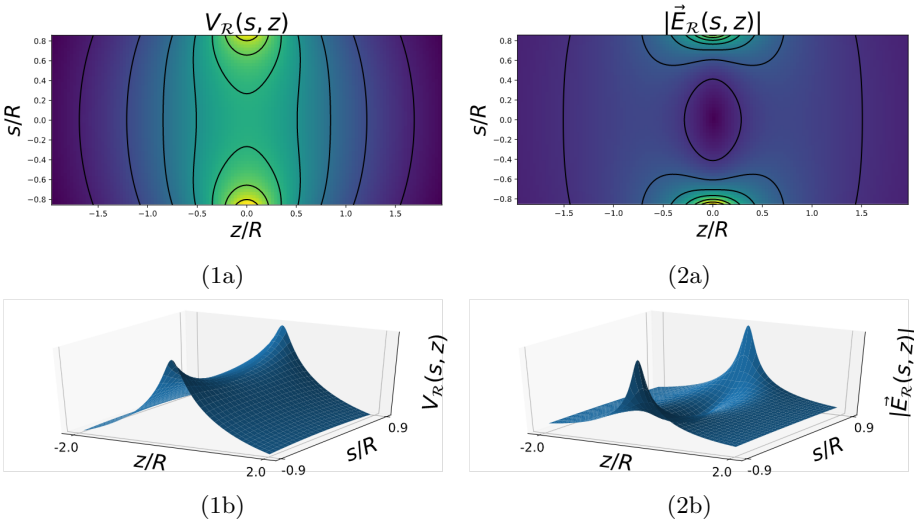

Figure 4: (1a) *Density plot of the electric potential, equation* (1)*;* (1b) *3D visualization of subfigure 1a;* (2a) *Density plot of the electric field strength, equation* (2)*;* (2b) *3D visualization of subfigure 2a. The electric field disappears at* $z = s = 0$*. Both graphs diverge at the ring position* ($z = 0$*;* $s = \pm R$)*.*

3.2 Ring Array Field

In the decelerator, every eighth ring of the array is electrically connected. Each ring can thus be recognized by two indices:

Period	σ:	$\{x \in \mathbb{Z}\}$	A period is a set of 8 consecutive rings.
Type	τ:	$\{x \in \mathbb{Z} \vert 0 \leq x \leq 7\}$	Every ring of the same type is connected.

The potential due to an individual ring on the array is then written as a translation and a modulation of equation (1)

$$V_{\sigma,\tau}(s,z) = a_\tau V_{\mathcal{R}}(s, z - (8\sigma + \tau)d), \tag{3}$$

with d the distance between two consecutive rings and $-1 \leq a_\tau \leq 1$ a parameter used to modulate the electric charge. Whenever an index is left out, a summation of this index is understood over its full domain. The full potential due to the array is thus expressed as

$$V_{,}(s,z) = \sum_{\sigma=-\infty}^{+\infty} \sum_{\tau=0}^{7} V_{\sigma,\tau}(s,z) = \sum_{\sigma=-\infty}^{+\infty} \sum_{\tau=0}^{7} a_\tau V_{\mathcal{R}}(s, z - (8\sigma + \tau)d). \tag{4}$$

The coefficients a_τ are tuned such that $V_,(s,z)$ matches the desired waveform as closely as possible. Since $\vec{\nabla}$ is a linear operator, the electric field is expressed in a form similar to equation (4) as

$$\vec{E}_,(s,z) = \sum_{-\infty}^{+\infty} \sum_{\tau=0}^{7} \vec{E}_{\sigma,\tau}(s,z) = \sum_{\sigma=-\infty}^{+\infty} \sum_{\tau=0}^{7} a_\tau \vec{E}_{\mathcal{R}}(s, z-(8\sigma+\tau)d). \tag{5}$$

For $a_\tau = \sin(\frac{\tau\pi}{4} - \omega t)|_{t=0}$, equations (4) and (5) are plotted in figure 5. This field resembles the configuration currently used in the Stark decelerator. The shape of one trap through one modulation (that is, from $\omega t = 0$ to $\omega t = \pi/4$ such that $a_\tau \to a_{\tau-1}$) is shown in figure 6.

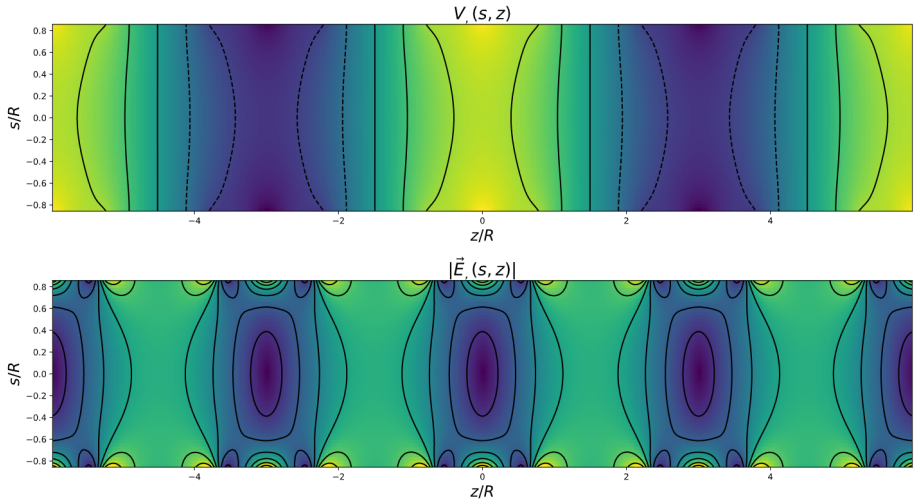

Figure 5: *Field configuration following equations* (4) *and* (5) *with* $a_\tau = \sin(\frac{\tau\pi}{4} - \omega t)$ *at* $t = 0$.

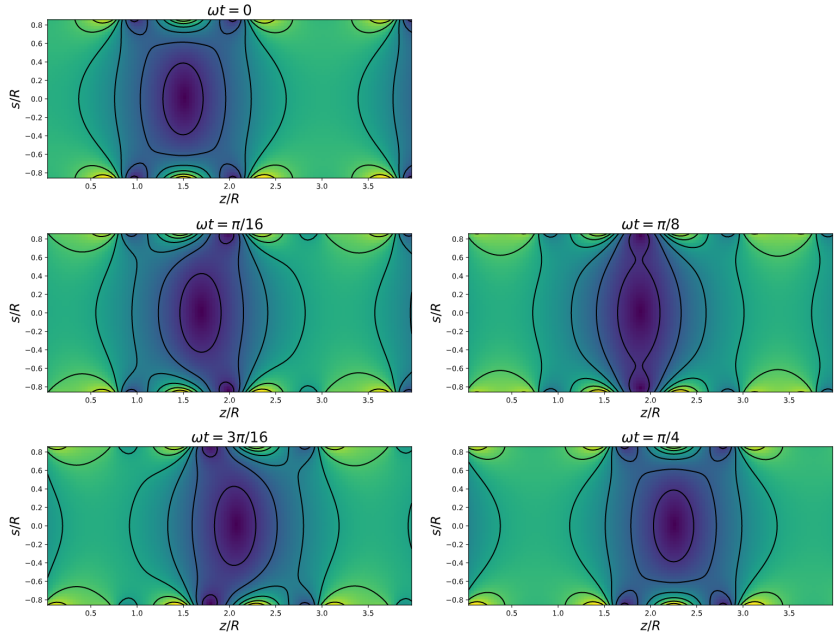

Figure 6: *Electric field through one modulation.*

3.3 Central Axis Field

On the central axis, the field of a single ring, given by equation (2), reduces to

$$V_{\mathcal{R}}(0,z) = \frac{\rho}{2\pi\epsilon_0}\int_0^{\pi}\frac{1}{\sqrt{R^2+z^2}}d\varphi = \frac{\rho}{2\epsilon_0}\frac{1}{\sqrt{R^2+z^2}}.$$

The field due to the zeroth ring type, according to equation (4), is given by

$$V_{,0}(0,z) = \sum_{\sigma=-\infty}^{+\infty} a_0 V_{\mathcal{R}}(0, z-8\sigma d).$$

By exploiting its periodicity every 8 rings, the field can be expanded into a Fourier series of the form[14]

$$\frac{1}{a_0}V_{,0}(0,z) = \frac{1}{2}p_0 + \sum_{n=1}^{+\infty} p_n \cos\frac{n\pi z}{4d}, \tag{6}$$

with the coefficients p_n given by

$$p_n = \frac{1}{4d}\int_{-4d}^{4d}\frac{1}{a_0}V_{,0}(0,z)\cos\frac{n\pi z}{4d}dz.$$

Solving for the coefficients p_n
Substituting the zeroth type potential into the integral gives

$$p_n = \frac{1}{4d}\int_{-4d}^{4d}\Big[\sum_{\sigma=-\infty}^{+\infty} V_{\mathcal{R}}(0, z-8\sigma d)\Big]\cos\frac{n\pi z}{4d}dz,$$

$$= \frac{1}{4d}\sum_{\sigma=-\infty}^{+\infty}\int_{-4d}^{4d} V_{\mathcal{R}}(0, z-8\sigma d)\cos\frac{n\pi z}{4d}dz.$$

Translating the integration variable $z \to z + 8\sigma d$ gives

$$= \frac{1}{4d}\sum_{\sigma=-\infty}^{+\infty}\int_{-4d+8\sigma d}^{4d+8\sigma d} V_{\mathcal{R}}(0, z)\cos\frac{n\pi z}{4d}dz,$$

where the cosine has remained unaffected since a shift of $8\sigma d$ means adding an integer multiple of 2π. Effectively, this integral evaluates patches of width $8d$ of the single ring potential. Putting together all patches into a single integral gives

$$= \frac{1}{4d}\int_{-\infty}^{+\infty} V_{\mathcal{R}}(0, z)\cos\frac{n\pi z}{4d}dz,$$

$$= \frac{\rho}{8d\epsilon_0}\int_{-\infty}^{+\infty}\frac{\cos\frac{n\pi z}{4d}}{\sqrt{R^2+z^2}}dz.$$

The integral can be rewritten by substitution of $uR \equiv z$ and $k \equiv \frac{n\pi R}{4d}$ as

$$= \frac{\rho}{8d\epsilon_0 R}\int_{-\infty}^{+\infty}\frac{\cos ku}{\sqrt{u^2+1}}du.$$

This equation has the form of the Modified Bessel Function of the Second Kind and order zero[22]. The coefficients p_n can thus be expressed using the Bessel function K_0 as

$$p_n = \frac{\rho}{4d\epsilon_0 R}K_0\big(\frac{n\pi R}{4d}\big). \tag{7}$$

Equation (7) has a decaying behaviour for $k \to \infty$, so for large n. This is nice, because it means that the central-axis field is mostly described by the first harmonics in the Fourier expansion. The function $K_0\big(\frac{n\pi R}{4d}\big)$ is plotted in figure 7 and the first 4 coefficients are marked using the configuration described in table 1.

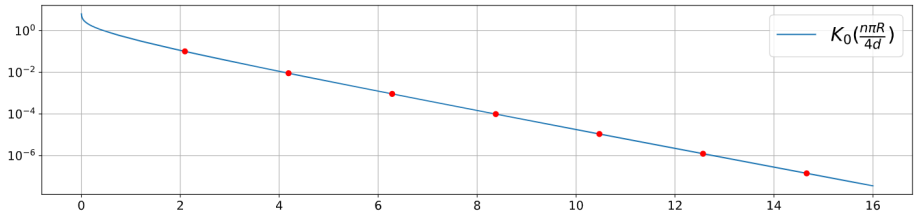

Figure 7: $K_0\left(\frac{n\pi R}{4d}\right)$ *with markers on the coefficients* $n = 1, ..., 8$ *using the ratio* $R/d = 4/3$ *as described in table 1.*

Central field expansion

The field of every other type can be obtained by translating equation (6):

$$\begin{aligned}
\frac{1}{a_\tau} V_{,\tau}(s,z) &= \frac{1}{a_0} V_{,0}(s, z - \tau d), \\
&= \frac{1}{2} p_0 + \sum_{n=1}^{+\infty} p_n \cos \frac{n\pi(z - \tau d)}{4d}, \\
&= \frac{1}{2} p_0 + \sum_{n=1}^{+\infty} p_n \left\{ \cos \frac{n\pi z}{4d} \cos \frac{n\pi\tau}{4} + \sin \frac{n\pi z}{4d} \sin \frac{n\pi\tau}{4} \right\}, \\
&= \frac{1}{2} p_0 + \sum_{n=1}^{+\infty} p_n \cos \frac{n\pi\tau}{4} \cos \frac{n\pi z}{4d} + \sum_{n=1}^{+\infty} p_n \sin \frac{n\pi\tau}{4} \sin \frac{n\pi z}{4d}.
\end{aligned}$$

By appropriate summation of the types, this means that the total (central) field can be written into a Fourier series expansion as

$$V_{,}(s,z) = \frac{1}{2} x_0 + \sum_{n=1}^{+\infty} x_n \cos \frac{n\pi z}{4d} + \sum_{n=1}^{+\infty} y_n \sin \frac{n\pi z}{4d}, \tag{8}$$

with the coefficients

$$x_0 = p_0 \sum_\tau a_\tau = 0, \tag{9}$$

$$x_n = p_n \sum_\tau a_\tau \cos \frac{n\pi\tau}{4}, \tag{10}$$

$$y_n = p_n \sum_\tau a_\tau \sin \frac{n\pi\tau}{4}. \tag{11}$$

A big note of caution is to be left at this point, which is that $p_0 \propto K_0(0) \to \infty$. This means that the electric potential will blow up unless $\sum_\tau a_\tau = 0$. However, since for any practical purposes the electric potential is invariant up to a spatial constant, one might as well choose the reference $p_0 = 0$ manually.

3.4 Analytic Field

In the previous subsection, the central axis field was described using a Fourier series expansion. This section will focus on generalizing that result to the full region between and through the rings[1].

By starting with the Laplace equation for potentials, it is found that in the absence of a charge

$$\nabla^2 V_{,}(s,z) = 0,$$

with $\nabla^2 V = \frac{1}{s}\partial_s V + \partial_s^2 V + \partial_z^2 V$ in cylindrical coordinates[2]. By rewriting $V_{,}(s,z) = V_{,}^{(s)}(s)V_{,}^{(z)}(z)$ using separation of variables, this gives

$$\begin{aligned}\nabla^2 V_{,} &= V_{,}^{(z)}\frac{1}{s}\partial_s V_{,}^{(s)} + V_{,}^{(z)}\partial_s^2 V_{,}^{(s)} + V_{,}^{(s)}\partial_z^2 V_{,}^{(z)} = 0,\\ \frac{1}{V_{,}^{(s)}}\frac{1}{s}\partial_s V_{,}^{(s)} &+ \frac{1}{V_{,}^{(s)}}\partial_s^2 V_{,}^{(s)} = -\frac{1}{V_{,}^{(z)}}\partial_z^2 V_{,}^{(z)} = k^2; \qquad \text{for some constant } k.\end{aligned}$$

Which leads to two ordinary differential equations

$$s\partial_s V_{,}^{(s)} + s^2\partial_s^2 V_{,}^{(s)} - s^2k^2 V_{,}^{(s)} = 0, \tag{12}$$

$$\partial_z^2 V_{,}^{(z)} + k^2 V_{,}^{(z)} = 0. \tag{13}$$

For a nonzero k, $V_{,}^{(z)}$ takes the general solution

$$V_{,}^{(z)}(z) = A\cos(kz) + B\sin(kz); \qquad \text{for some constants } A \text{ and } B.$$

The periodicity of the potential every eight electrodes, $V_{,}^{(z)}(z) = V_{,}^{(z)}(z+8d)$ put a constraint on k

$$\begin{aligned}kz + 2\pi n &= kz + 8kd,\\ k &= \frac{n\pi}{4d}; \qquad n \in \mathbb{Z}.\end{aligned}$$

Meanwhile, the differential equation for s has the form of the Modified Bessel Differential Equation[20]. Its solution is then proportional to the Modified Bessel Function of the First Kind and order zero[3][21]:

$$\begin{aligned}V_{,}^{(s)}(s) &= CI_0(sk); \qquad \text{for some constant } C,\\ &= C\sum_{p=0}^{+\infty}\frac{(\frac{1}{2}sk)^{2p}}{(p!)^2}.\end{aligned}$$

[1] The following derivations were inspired by [17].

[2] $V(s,z)$ gives $\nabla^2 V = \frac{1}{s}\partial_s(s\partial_s V) + \frac{1}{s^2}\partial_\varphi^2 V + \partial_z^2 V = \frac{1}{s}\partial_s V + \partial_s^2 V + \partial_z^2 V$.

[3] Actually, the general solution is a linear combination of the Modified Bessel Function of the First and Second kind. However, the second kind diverges as $(s \to 0)$[22], which is assumed not to be the case. (This assumption is also supported by the numerically obtained solutions shown in figure 5.)

The full solution of the field is then given by a linear combination of the solutions with unique k^4:

$$V_{,}(s,z) = A_0 + \sum_{n=1}^{+\infty} A_n I_0\big(\frac{n\pi s}{4d}\big)\cos\frac{n\pi z}{4d} + \sum_{n=1}^{+\infty} B_n I_0\big(\frac{n\pi s}{4d}\big)\sin\frac{n\pi z}{4d}. \tag{14}$$

On the central axis ($s = 0 \implies I_0(0) = 1$), equation (14) reduces to

$$V_{,}(0,z) = A_0 + \sum_{n=1}^{+\infty} A_n \cos\frac{n\pi z}{4d} + \sum_{n=1}^{+\infty} B_n \sin\frac{n\pi z}{4d}.$$

This happens to be the exact same form found in section (3.3), equation (4). Its coefficients are given by equations (9), (10) and (11). Substituting the coefficients $A_0 = x_0 = 0$, $A_n = x_n$ and $B_n = y_n$ back into equation (14) gives the full field inside the decelerator

$$V_{,}(s,z) = \frac{\rho}{4d\epsilon_0 R}\sum_{n=1}^{+\infty} K_0\big(\frac{n\pi R}{4d}\big)I_0\big(\frac{n\pi s}{4d}\big)\sum_{\tau=0}^{7} a_\tau\Big\{\cos\frac{n\pi\tau}{4}\cos\frac{n\pi z}{4d} + \sin\frac{n\pi\tau}{4}\sin\frac{n\pi z}{4d}\Big\}.$$

Using trigonometry, the field can be rewritten into the final form

$$V_{,}(s,z) = \frac{\rho}{4d\epsilon_0 R}\sum_{n=1}^{+\infty} K_0\big(\frac{n\pi R}{4d}\big)I_0\big(\frac{n\pi s}{4d}\big)\sum_{\tau=0}^{7} a_\tau\cos\left(\frac{n\pi(z-\tau d)}{4d}\right). \tag{15}$$

Electric Field

The electric field is obtained by taking the negative gradient of equation (15) in cylindrical coordinates:

$$\begin{aligned}
E_{,}^{(s)}(s,z) &= +\frac{\rho}{4d\epsilon_0 R}\sum_{n=1}^{+\infty} K_0\big(\frac{n\pi R}{4d}\big)I_1\big(\frac{n\pi s}{4d}\big)\frac{n\pi}{4d}\sum_{\tau=0}^{7} a_\tau\cos\left(\frac{n\pi(z-\tau d)}{4d}\right),\\
E_{,}^{(z)}(s,z) &= -\frac{\rho}{4d\epsilon_0 R}\sum_{n=1}^{+\infty} K_0\big(\frac{n\pi R}{4d}\big)I_0\big(\frac{n\pi s}{4d}\big)\frac{n\pi}{4d}\sum_{\tau=0}^{7} a_\tau\sin\left(\frac{n\pi(z-\tau d)}{4d}\right),\\
\vec{E}_{,} &= E_{,}^{(s)}\hat{s} + E_{,}^{(z)}\hat{z}.
\end{aligned} \tag{16}$$

Where $I_1(x)$ is the Modified Bessel Function of the First Kind and first order. It is related to the zeroth order I_0 through

$$I_n(x) = T_n(\partial_x)I_0(x),$$

with $T_n(x)$ the Chebyshev polynomial of the first kind[19]. For $n = 1$, $T_1(x) = x$ such that $I_1(x) = \partial_x I_0(x)$ simply becomes the first derivative.

[4]Note that $I_0\big(\frac{n\pi z}{4d}\big)\big|_{n=0} = 1$ and $I_0(x) = I_0(-x)$, such that a summation over $n \in \mathbb{N}$ suffices.

A note about the boundary fields

Equations (15) and (16) hold under the assumption that there are sufficiently many rings ahead of and behind the current position on the decelerator. At the boundaries, the field will get distorted and it will drop off exponentially. However, for most practical use of equations (15) and (16) this is not so much an issue. The reason for this is that the decelerator is turned on when the particles are already sufficiently far into the tube such that they do not experience any boundary fields.

4 Effective Field

The full effective field as experienced by the particles is rather complex. For a proper description, the internal quantum mechanical properties of the atom or molecule in question need to be specified. However, up to a certain level they can still be discussed in a more generalized framework. The aim of this section is to investigate the effective potentials and forces that act on the particles.

4.1 Stark Effect - Classical View

For most analysis in this report, a classical view on the Stark effect suffices. As will be shown in section 4.2, the quantum mechanical description through degenerate perturbation theory will fall back to the classical result under a few feasible approximations.

For the classical model, some charge distribution ρ is considered to be in the presence of an electric potential V. The energy of the system (due to the external field) is then given by the integral

$$\mathcal{E} = \int \rho(\vec{r}) V(\vec{r}) d^3r.$$

As is derived in section 7.1, the electric potential can be recast into a series expansion around the center of the distribution as

$$\begin{aligned} V(\vec{r}) = V(\vec{r}_0 + \vec{a}) &= e^{\vec{a}\cdot\vec{\nabla}} V(\vec{r}_0), \\ &\approx V(\vec{r}_0) + \vec{a}\cdot\vec{\nabla}V(\vec{r}_0) + ..., \\ &= V(\vec{r}_0) - \vec{a}\cdot\vec{E}(\vec{r}_0) + ..., \end{aligned}$$

where $\vec{E} = -\vec{\nabla}V$ gives the corresponding electric field. Substituting this back into the energy intergral gives

$$\begin{aligned} \mathcal{E} &\approx \int \rho(\vec{r}) V(\vec{r_0}) d^3r - \int \rho(\vec{r}) \vec{a}\cdot\vec{E}(\vec{r}_0) d^3r, \\ &= V(\vec{r}_0) \int \rho(\vec{r}) d^3r - \left(\int \rho(\vec{r}) \vec{a}\, d^3r \right) \cdot \vec{E}(\vec{r}_0), \\ &= QV - \vec{P}\cdot\vec{E}. \end{aligned}$$

The first term gives the zero energy of the particle. Unless the particle is charged, this term will be zero. The second term gives a relation between the electric dipole moment $\vec{P}$ of the particle and the external field $\vec{E}$. This term gives a simplified expression for the first order Stark energy:

$$\mathcal{V}_S = -\vec{P}\cdot\vec{E} = (\vec{P}\cdot\vec{\nabla})V. \tag{17}$$

4.2 Stark Effect - Quantum Mechanical View

Although it helps with building a general picture, the classical derivation of the Stark energy in section 4.1 has its flaws. For instance, equation (17) does not directly support the existence of LFS states. LFS states would suggest a negative $\vec{P}$. However, in the classical view, this will result in a torque causing the particle to reorient itself with the external field until it does reach a HFS configuration. To properly explain the existence of LFS states, the use of quantum mechanics becomes necessary.

When present in an electric field, the electronic orbitals of an atom or molecule are deformed, causing its energy levels to shift and degenerate states to split. In general, a particle of charge q due to an electric field $\vec{E}$ experiences a force $\vec{F} = q\vec{E}$. The corresponding energy is found by integrating the force over the displacement of the particle. Assuming an external field pointing in the $\hat{z}$ direction, this gives

$$\mathcal{E} = -\int \vec{F} \cdot d\vec{l} = -\int qE_z dz = -qE_z z,$$

where the particle is assumed to be sufficiently small such that E becomes a constant over the integral. This means that the Hamiltonian obtains a perturbation of the form

$$H'_S = -qE_z z.$$

According to equation (43), derived in appendix 7.2, the energy levels of a k-fold degenerate state will split into

$$\mathcal{E}_i^{(1)} = \sum_{j=1}^{k} \frac{a_j}{a_i} \langle \psi_i^{(0)} | \, H'_S \, | \psi_j^{(0)} \rangle \, . \tag{18}$$

When the degeneracy $k = 1$, as is often the case for molecules, equation (18) reduces to

$$\mathcal{E}^{(1)} = \langle \psi^{(0)} | - qE_z z \, | \psi^{(0)} \rangle = -q \, \langle \psi^{(0)} | \, z \, | \psi^{(0)} \rangle \, E_z = -q \langle z \rangle E_z,$$

where $\langle z \rangle$ denotes the expectation value of z, the position of the particle. The total energy shift is then found by summing the individual charged components of the particle. This gives

$$\sum_i -q_i \langle z \rangle_i E_z = -\Big(\sum_i q_i \langle z \rangle_i \Big) E_z = -P_z E_z = -\vec{P} \cdot \vec{E},$$

which matches the result found through the classical approach, equation (17).

4.3 Particle Waterslide

In the simplified model, equation (17) says that the effective field experienced by a particle becomes linear to the electric field itself. In that case, figures 5 and 6 give a good visualization of the effective fields. With the addition that the bases may be stretched, squeezed or inverted depending on the direction of $\vec{P}$.

In section 5 the behaviour of a particle is considered from a frame of reference that is fixed to the traveling waves. Since these waves decelerate, the frame is of non-inertial kind. Because of this, the effective field gains an additional inertial force $F_I = -ma$, with m the mass of the particle and a the acceleration of the frame. To this force, an effective potential can be assigned of the form

$$\mathcal{V}_I(z) = -\int F_I dl = maz. \tag{19}$$

The total effective potential experienced by the particles is then given by combining equations (16), (17) and (19). Doing so gives

$$\mathcal{V}(s,z) = \mathcal{V}_I(z) + (\vec{P}\cdot\vec{\nabla})V_,(s,z) = maz - \vec{P}\cdot\vec{E}_,(s,z). \tag{20}$$

An important note is to be left at this point, and that is that the dependence of the polarization $\vec{P}$ on the external field heavily affects the resulting shape of equation (20).

The term maz causes the effective field to tilt, making it look like a bumpy waterslide where particles slide down to the lowest energy. Either they will then diverge to the global minimum or get stuck at a local one. Particles of the latter case are called stable, as they remain confined within their respective trap. Some simplified shapes of this waterslide are discussed for different scaling behaviours of $\vec{P}$ on the external field. The examples assume that the particles do not rotate, and that they are anti-aligned with the external field as to describe a LFS state. (HFS states are described in the same way, with an additional minus sign. This amounts to flipping the waterslide upside-down.)

4.3.1 Static Polarization

The most simple situation is described by a static $\vec{P}$. This represents the permanent dipole moment of a sturdy particle, which does not get affected by the external field. When $\vec{P}$ is a constant, one cannot really speak of Stark shift since the energy levels do not shift. The Stark energy from equation (17) becomes directly proportional to the external field. The effective field for this case is shown in figure 8a. It is to be noted that since a static polarization was chosen that is always anti-aligned with the external field (LFS), a discontinuity in the derivative is observed at the central-axis.

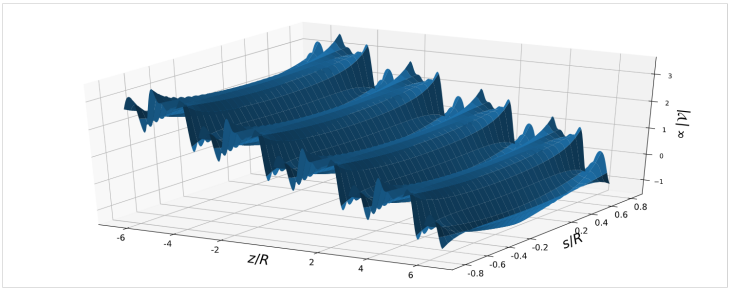

(a) $|\vec{P}| = constant$

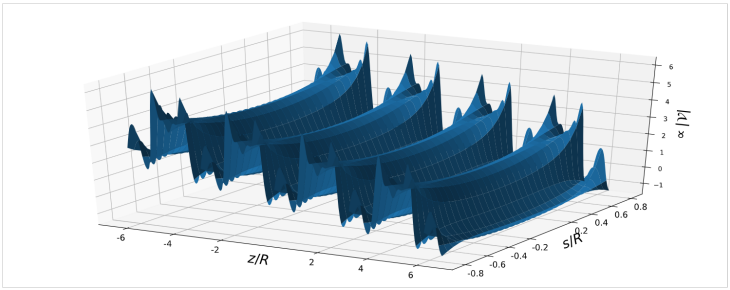

(b) $|\vec{P}| \propto |\vec{E}_{,}|$

Figure 8: *Particle waterslides following a static and a linear polarization. Depending on the initial velocity and position of a particle, it will either get stuck in a local minimum (trap) or slide down indefinitely.*

4.3.2 Linear Polarization

In the situation where the polarization $\vec{P}$ is mostly linearly proportional to the external field, as is the case for linear dielectrics, the Stark energy becomes quadratic to the external field:

$$\mathcal{V}_S(s,z) = maz - \vec{P} \cdot \vec{E}_{,}(s,z) = maz - \epsilon_0 \chi_e E_{,}^2(s,z), \quad \text{for some constant } \chi_e.$$

The effective potential fitting a linear polarization is shown in figure 8b. As can be seen, compared to the static case, the waves become much more pronounced. This has the result that linear particles can be decelerated much faster than statically polarized particles. (Increasing the deceleration/acceleration amounts to tilting the graph further.)

4.3.3 BaF Field

A more realistic example can be illustrated using the energy levels of barium-fluoride. Figure 9 shows the energy of several levels as a function of the external field strength. Note that only the $|1,0\rangle$, $|2,1\rangle$ and $|2,2\rangle$ states have a LFS component. These components can be used to decelerate the molecule in the

decelerator.

In figure 9c, the maximum electric field strength at $s/R = 0.8$ was set to match that at the maximum of the $|1, 0\rangle$ curve in figure 9a. The smooth start of the curve causes regions of low field strength to take the same energy. As a result, the trap size becomes stretched. Meanwhile, around the maximum of the curve the energy becomes (almost) constant for a while. This explains the seemingly constant energy between two consecutive traps in figure 9c.

If the overall electric field strength is set to be too high, HFS components of the Stark curve will start to drop within the range of the field. This has the effect of decreasing the stability. Similarly, due to the flat start of the LFS states a field that is too weak will cause the barrier between traps to decrease in height. This also has the effect of reducing the stability.

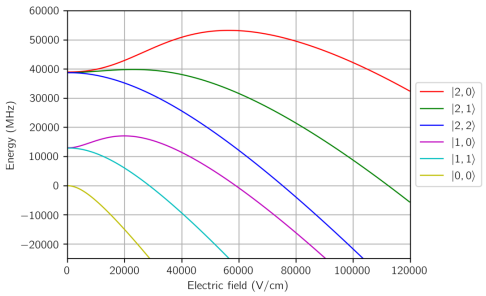

(a) *Energy levels in BaF[12].*

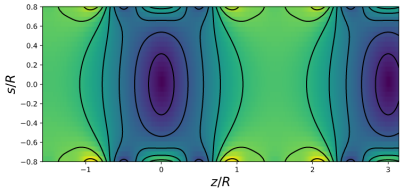

(b) *Electric field strength.*

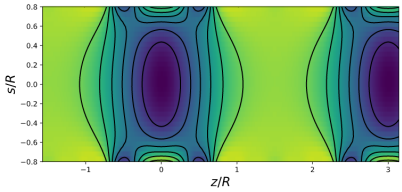

(c) *Effective field corresponding to the* $|1, 0\rangle$ *state.*

Figure 9: *Stark energy in bariumfluoride.*

5 One-Dimensional Motion

In this section statically polarized particles are considered that are fixed to the central axis and due to a perfect harmonic field. Despite these seemingly radical approximations, many of key characteristics regarding behaviour and stability of the particles can be explained.

5.1 Equation of Motion

In constructing the equation of motion, a frame of reference will be used that is fixed to the traveling waves of the decelerator. The total effective potential is given by equation (20). Combined with the kinetic energy of a particle of mass m, this gives the Lagrangian

$$\mathcal{L} = \frac{1}{2}m\dot{z}^2 - P_z\partial_z V_{,}(z) - maz. \tag{21}$$

The equation of motion is then found by solving the Euler-Lagrange equation $[d_t\partial_{\dot{z}} - \partial_z]\mathcal{L} = 0$:

$$m\ddot{z} + P_z\partial_z^2 V_{,}(z) + ma = 0. \tag{22}$$

5.1.1 Phase Position

In analyzing the equation of motion, it is more convenient not to talk of the position z, but rather about the relative phase ϕ with respect to the surrounding wave. The phase ϕ of a particle is obtained by re-scaling the z axis following

$$\phi \equiv \frac{2\pi}{\lambda}z; \quad z = \frac{\lambda}{2\pi}\phi.$$

This means the differentials are adjusted accordingly

$$d_\phi \equiv \frac{d}{d\phi} = \frac{d}{\frac{2\pi}{\lambda}dz} = \frac{\lambda}{2\pi}dz; \quad d_z = \frac{2\pi}{\lambda}d_\phi.$$

And also the dipole moment will need a makeover as to give

$$P_\phi \equiv \frac{2\pi}{\lambda}P_z.$$

Rewriting the equation of motion, equation (22), using the phase position rather than z gives

$$\frac{m\lambda^2}{4\pi^2}\ddot{\phi} + P_\phi\partial_\phi^2 V_{,}(\phi) + \frac{ma\lambda}{2\pi} = 0. \tag{23}$$

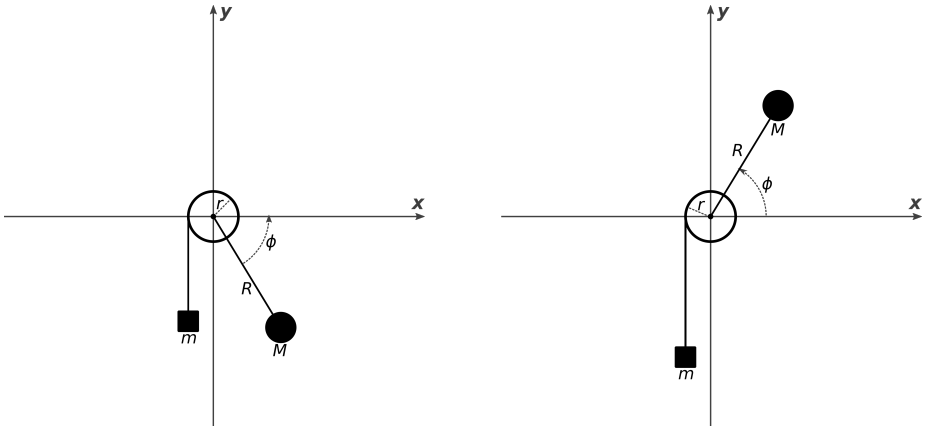

Figure 10: *A biased pendulum with a rigid bob of length R and a mass M at its and. The pendulum has a string wrapped around its axis of rotation, at radius r, and a second mass m suspended at one end of the string. The rod and the string are considered to be massless.*

5.1.2 First Harmonic

As a first approximation, the electric potential will be described by a single harmonic of wavelength $\lambda = 8d$. The effective field from equation (20) then becomes

$$\mathcal{V}(\phi) = \frac{ma\lambda}{2\pi}\phi - V_0 P_\phi \sin\phi, \tag{24}$$

and the equation of motion takes the form

$$\frac{m\lambda^2}{4\pi^2}\ddot{\phi} - V_0 P_\phi \cos\phi + \frac{ma\lambda}{2\pi} = 0. \tag{25}$$

5.2 Biased Pendulum

In turns out that the equation of motion (25) is isomorphic to the equation of motion of a biased pendulum[5]. That is, a regular pendulum with a string wrapped around its axis of rotation and a mass hanging down one end of the string. The pendulum itself consists of a rigid bob with another mass placed at its end. A schematic is shown in figure 10.

The pendulum is confined to move on the xy-plane, which gives the system 2 degrees of freedom. However, since $x^2 + y^2 = R^2$, one degree drops out leaving the system one-dimensional. Just the angle ϕ is enough to describe the full state of the pendulum. So before going into the equation of motion, it is worth to first express the coordinates (x_M,y_M,x_m,y_m) and their derivatives in terms of ϕ following the orientation of figure 10:

$$
\begin{aligned}
x_M &= R\cos\phi \quad &;\quad \dot{x}_M &= -R\dot{\phi}\sin\phi,\\
y_M &= R\sin\phi \quad &;\quad \dot{y}_M &= R\dot{\phi}\cos\phi,\\
& \quad &;\quad \dot{x}_m &= 0,\\
y_m &= -r\phi + y_{m,0} \quad &;\quad \dot{y}_m &= -r\dot{\phi}.
\end{aligned}
$$

The kinetic and potential energy of the pendulum are then given by

$$
\begin{aligned}
\mathcal{K}_M &= \frac{1}{2}M(\dot{x}_M^2 + \dot{y}_M^2) = \frac{1}{2}MR^2\dot{\phi}^2,\\
\mathcal{V}_M &= Mgy_M = MgR\sin\phi.
\end{aligned}
$$

For the bias, these energies are given by[5]

$$
\begin{aligned}
\mathcal{K}_m &= \frac{1}{2}m(\dot{x}_m^2 + \dot{y}_m^2) = \frac{1}{2}mr^2\dot{\phi}^2,\\
\mathcal{V}_m &= mgy_m = -mgr\phi.
\end{aligned}
$$

Combining the energies gives the Lagrangian

$$
\mathcal{L} = \frac{1}{2}(MR^2 + mr^2)\dot{\phi}^2 - MgR\sin\phi + mgr\phi. \tag{26}
$$

Solving the Euler-Lagrange equation $[d_t\partial_{\dot{\phi}} - \partial_\phi]\mathcal{L}$ gives the equation of motion

$$
(MR^2 + mr^2)\ddot{\phi} + MgR\cos\phi - mgr = 0. \tag{27}
$$

5.2.1 Isomorphism of the Equation of Motion

Both the equation of motion of a particle in the decelerator (equation (25)) as well as that of the biased pendulum (equation (27)) are of the form

$$
A\ddot{\phi} + B\cos\phi - C = 0, \tag{28}
$$

with positive constants A, B and C for LFS states ($P_\phi < 0$) in a decelerator ($a < 0$). By comparing the equations of motion[6]

$$
(MR^2 + mr^2) \sim \frac{m'\lambda^2}{4\pi^2} = A, \tag{29}
$$

$$
MgR \sim -V_0 P_\phi = B, \tag{30}
$$

$$
mgr \sim -\frac{m'a\lambda}{2\pi} = C, \tag{31}
$$

it can be seen that both systems are effectively described by a perturbed pendulum. Indeed, setting $m = 0$ and $a = 0$ both have the same effect by turning

[5] Actually there should be a factor $mgy_{m,0}$ added to the potential energy to take care of the zero-length energy of the bias. However, since the Lagrangian and as such the equation of motion both depend only on the derivative of the energy, I will sneak this constant to zero.

[6] The mass of the particle in the decelerator here will be written as m' instead of m as to not confuse it with the mass of the bias in the biased pendulum.

the equations of motion into a simple harmonic oscillator problem. So the effect of including the bias to the biased pendulum is what describes the inertial force in the non-inertial frame of the wave.

The potential energy from equation (24) is then give by

$$\mathcal{V}(\phi) = B\sin\phi - C\phi. \tag{32}$$

Or for a more generalized potential:

$$\mathcal{V}(\phi) = B\partial_\phi \tilde{V}_{,}(\phi) - C\phi, \tag{33}$$

where $\tilde{V}_{,}(\phi) = \frac{1}{V_0}V_{,}(\phi)$ is the normalized potential. The kinetic energy is expressed as

$$\mathcal{K}(\dot{\phi}) = \frac{1}{2}A\dot{\phi}^2. \tag{34}$$

5.2.2 Alternative Orientations

Although equation (27) can be used to describe the behaviour of particles in LFS as well as HFS in both a decelerator or an accelerator, additional orientations exist to make the isomorphism more intuitive. From equation (31) it can already be guessed that going from a decelerator ($a < 0$) to an accelerator ($a > 0$) amounts to turning the bias mass m or the radius r negative. A similar reasoning can be used with equation (30) where a HFS state amounts to flipping the sign of P_ϕ. In order for the pendulum to make for a sensible analogy, m, M, r and R all need to be positive. (Imagining a negative mass or negative radius puts away with the intuition.)

What it means to change from a decelerator to an accelerating configuration is to flip the direction of the inertial/bias force, equation (31). Placing the bias at the other end of the pendulum ensures that the pendulum has again all positive parameters.

Changing the particles from LFS states to HFS states amounts to flipping the sign of the restoring force, equation (30). This can be achieved by a change of basis $\phi \to -\phi$ since this will flip the sign of the second term in equation (27). This basis transformation keeps the rest of the equations invariant, except for the bias potential energy[7]. So when changing from a LFS configuration to a HFS state, the bias must also be placed at the other end of the pendulum.

An overview of the different pendulum orientations and their corresponding configurations for the decelerator/accelerator are given in figure 11. Their equations of motion are given by equation (28) where A, B and C are found in table 2.

[7]Note that the kinetic energies depend only on the square.

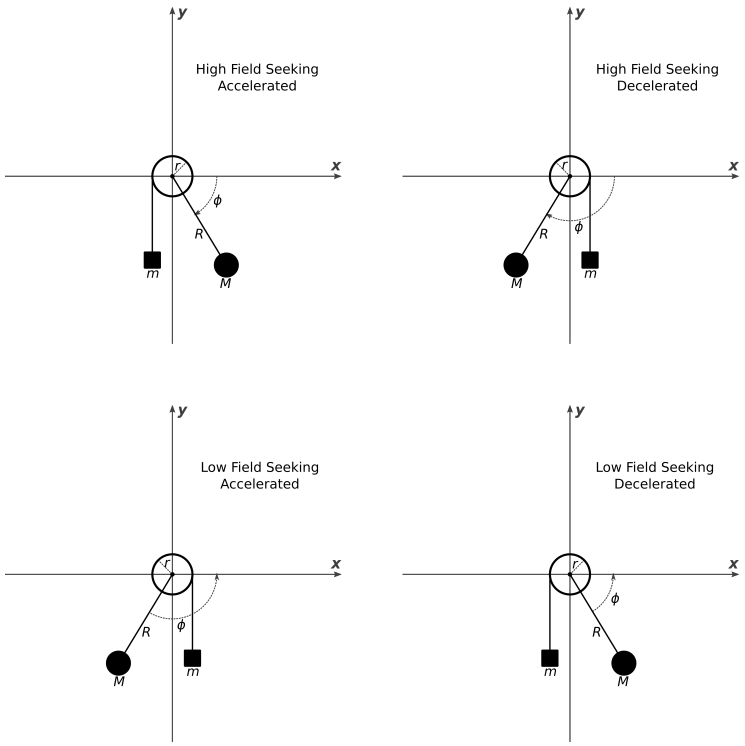

Figure 11: *Four orientations of the biased pendulum to fit the different configurations of the accelerator/decelerator. The orientations are chosen as to make their isomorphism intuitively fitting.*

5.3 Phase Stability

In the following analysis, a two-dimensional phasespace will be considered using the phase and its derivative (ϕ, $\dot{\phi}$). According to Liouville's theorem[15], in a system where the forces are determined solemnly by a potential as a function of position, the phasespace particle density remains constant. This has the consequence that two particle trajectories in phasespace never cross. If two different particles share the same phasespace coordinates at some different time, then these particles are equivalent up to a translation in time.

5.3.1 Equilibrium States

Just like an ordinary, non-biased pendulum, the biased pendulum has two equilibrium points. A stable and an unstable one. This corresponds to two particles of constant phase per wavelength in the decelerator. These points can be found

		A	B	C
LFS	Decelerated	$(MR^2 + mr^2)$	MgR	mgr
LFS	Accelerated	$(MR^2 + mr^2)$	MgR	$-mgr$
HFS	Decelerated	$(MR^2 + mr^2)$	$-MgR$	$-mgr$
HFS	Accelerated	$(MR^2 + mr^2)$	$-MgR$	mgr

Table 2: *terms corresponding to A, B and C for different orientations of the biased pendulum.*

by setting $\dot{\phi} = 0$ and $\ddot{\phi} = 0$ in the equation of motion (28):

$$B\cos\phi - C = 0 \quad \Longrightarrow \quad \cos\phi = \frac{C}{B},$$

which has solutions for

$$\phi_1 = \cos^{-1}\frac{C}{B} = \cos^{-1}\frac{ma\lambda}{2\pi V_0 P_\phi},$$
$$\phi_2 = 2\pi - \phi_1.$$

One of these determines the stable and the other the unstable equilibrium. Which becomes which depends on the sign of a and P_ϕ. (That is, LFS/HFS and deceleration/acceleration.) From this moment, the stable equilibrium will be referred to as ϕ_s and the unstable or tipping point using $\phi_u = 2\pi - \phi_s$.

5.3.2 One-Dimensional Traps

For particles whose initial velocity is zero, the stability can be directly derived by looking at the potential. The total potential energy in the decelerator is given by equation (32):

$$\begin{aligned}\mathcal{V} &= B\sin\phi - C\phi,\\ \frac{1}{B}\mathcal{V} &= \sin\phi - \frac{C}{B}\phi,\\ &= \sin\phi - \phi\cos\phi_1. \end{aligned} \tag{35}$$

Equation (35) looks like a sine that is slightly tilted. Actually, this is precisely what was shown in section 4.3 where the full three-dimensional potential was shown to be a tilted wave. Equation (35) is plotted in figure 12. A particle with initial phase ϕ_0 is stable if it lies between two local maxima whose energy is higher than that at ϕ_0. When tracking the motion of the particle, it will either oscillate in a local minimum (stable) or slide down indefinitely (unstable).

The equilibrium points split each wavelength into two regions, a stable and an unstable region. The size of these regions depends on the inclination $\cos\phi_1 = \frac{C}{B}$, which depends on the acceleration a/the mass of the bias m (equation (31)). If there is no acceleration, the slope disappears and the system acts like a normal

pendulum (see figure 12, $\phi_s = \frac{1}{2}\pi$). But when the acceleration is too large ($\sim$ the bias is too heavy), any local minima will disappear and particles will be bound to slide forever (see figure 12, $\phi_s = 0$).

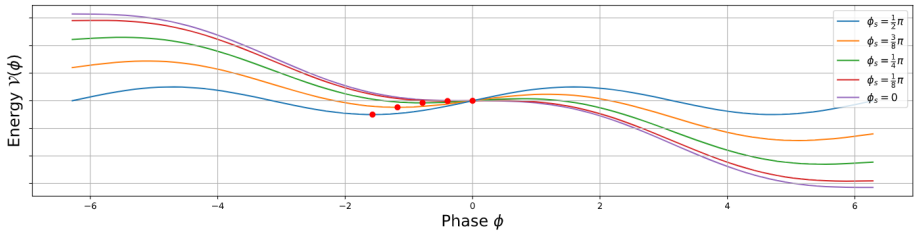

Figure 12: *Total potential energy in the biased pendulum as a function of ϕ. Stable equilibria for $\phi \in [0, 2\pi]$ are marked by red dots.*

5.3.3 Phasespace Trajectories

As a final extension to complete the one-dimensional stability, particles with non-zero initial velocity are considered. As mentioned in the opening of this subsection, through Liouville's theorem, two particle trajectories never cross. This means that any particle with non-zero initial velocity can be related to a particle with zero initial velocity by means of a time translation. The moment when a particle has zero velocity is called the turning point. In figure 13, a flowmap is shown of the phasespace trajectories. Shown in red is the separatrix, the boundary between the stable and unstable regions in phasespace. Figure 14 shows the same graph for different values of the acceleration. Both graphs were drawn by numerical integration of the equation of motion (28) with $C \propto a$.

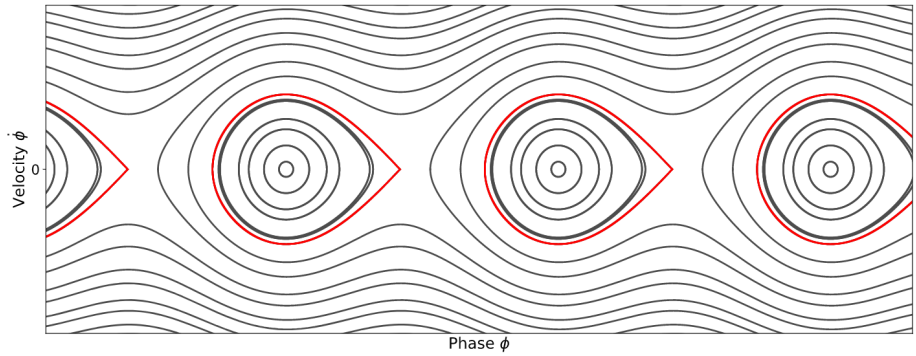

Figure 13: *Some particle trajectories in $(\phi, \dot{\phi})$ phasespace. Shown in red is the separatrix, which is the boundary between stable and unstable regions. Particles in the bottom half ($\dot{\phi} < 0$) will propagate left and particles on the top half ($\dot{\phi} > 0$) follow the contour lines right.*

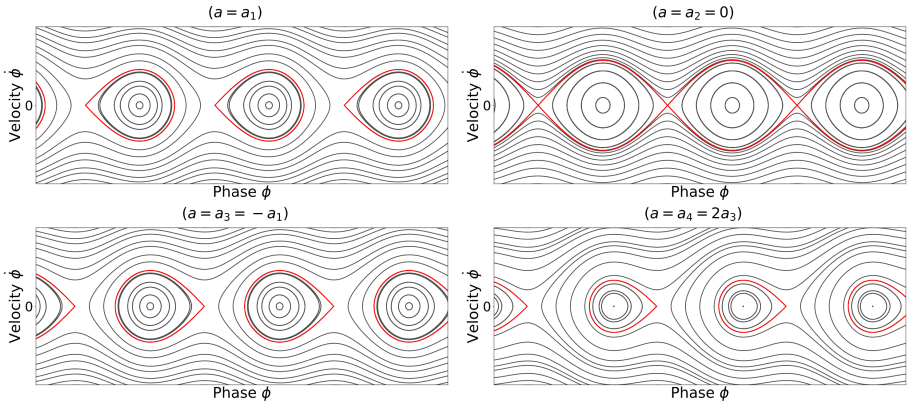

Figure 14: *Some particle trajectories in* $(\phi, \dot{\phi})$ *phasespace. The acceleration is varied in each plot following* $a_1 > 0 > a_3 > a_4$*. As the absolute value of the acceleration increases, the separatrix (and as such the region of stability) grows smaller.*

From figures 13 and 14 it can be seen that every path crosses the $(\dot{\phi} = 0)$ axis at least once. The crossing is called the turning point. Every particle can be related to a turning point either by a positive time translation or a (hypothetical) negative one, even if the particle in reality has never reached these coordinates.

To mathematically determine whether a particle is stable or not, consider a particle at the phasespace coordinates $(\phi, \dot{\phi})$. Its energy is given by

$$\mathcal{E}(\phi, \dot{\phi}) = \mathcal{K}(\dot{\phi}) + \mathcal{V}(\phi) = \frac{1}{2} A \dot{\phi}^2 + C\phi - B \sin \phi.$$

Since the total energy is conserved[8], this gives

$$\dot{\phi}^2 = \frac{2}{A} \big[\mathcal{E} - C\phi + B \sin \phi \big]. \tag{36}$$

Equation (36) essentially describes the flow of a particle with energy $\mathcal{E}$ in $(\phi, \dot{\phi})$ phasespace. Its graph is symmetric through $\dot{\phi} = 0$. The paths with equal energy may be defined on several intervals. If the interval is closed, the path has to return to itself and is therefore stable. However, if the path is open on one end, the path is able to diverge and the particle is unstable.

To take as example the path of a particle with total energy $\mathcal{E} = 0$, which is

[8] In the non-inertial frame of the wave, at least.

defined when

$$-C\phi + B\sin\phi > 0,$$
$$\sin\phi > \phi\cos\phi_1. \tag{37}$$

In the case that $\cos\phi_1 = \frac{C}{B} = -0.12$, the graph is defined on three intervals; two closed (stable) intervals and one open (unstable) one. These paths are illustrated in figure 15.

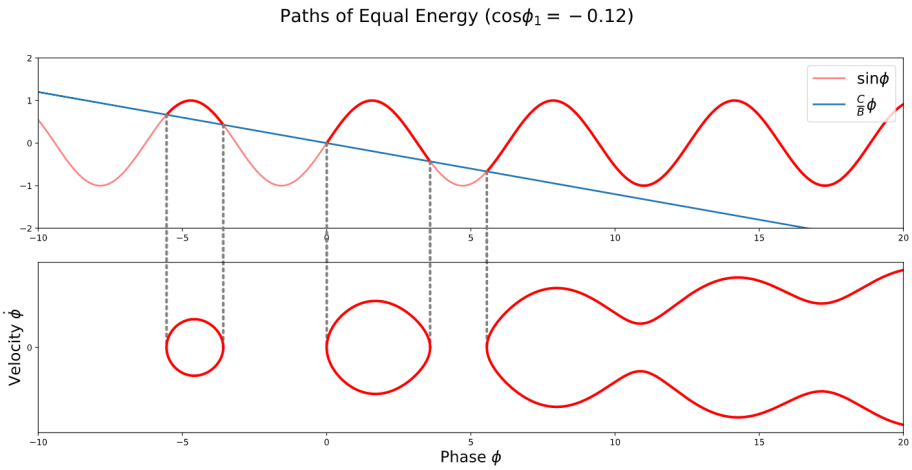

Figure 15: *Phasespace trajectories drawn for three paths with the same energy following equations* (36) *and* (37).

6 Conclusion

In conclusion, for this project the aim was to find and describe analytic models for the fields and behaviour of molecules in a traveling-wave Stark decelerator. Finding such models began by studying the working principles of a Stark decelerator as well as some fundamental statements regarding stability of states and Earnshaw's theorem.

An analytic description was found for the electric potential and the electric field. By making use of a Fourier series expansion in combination with Laplace's equation in cylindrical coordinates, a vectorfield expression for the electric field was found. The only approximation taken in this model is for the ring thickness to be negligible.

Using the electric field and a simplified expression for the Stark energy, the effective fields were discussed as experienced by the particles. For particles fixed to the central-axis, the behaviour of a particle seems to become similar to that of an oscillator. By approximating the field to be harmonic, the problem becomes isomorphic to a biased pendulum. Using this analogy some of the phas-espace stability features were discussed. These features are expected to help in understanding the three-dimensional stability.

6.1 Outlook

The analytic analysis is however far from finished. With the limited amount of time granted to this project, many questions and applications remain unexplored. As a continuation of this project, several improvements/extensions can be made to the current analysis.

One such improvement would be to look for approximations of the field equation as to make it computationally more friendly. (For instance, the Bessel function in figure 7 seems mostly linear along the coefficients.) It would also be worth to look into the difference between the field equation (16) and numerical results that do take into account the finite thickness of the electrodes. The project can be extended by continuing the stability analysis up to three dimensions.

The models described in this project can be used to improve the efficiency and accuracy of simulations. Many of the pictures used in this project as well as numerical validation of the models was done by means of parallel computation on a graphics card. Currently, simulations on the Stark decelerator are performed using a combination of C and Python[13]. It is expected that computational time can be greatly decreased not only by replacing some numerical parts with analytic descriptions, but also by introducing parallel computational methods.

References

[1] Parul Aggarwal, Hendrick L. Bethlem, Anastasia Borschevsky, Malika Denis, Kevin Esajas, Pi A. B. Haase, Yongliang Hao, Steven Hoekstra, Klaus Jungmann, Thomas B. Meijknecht, Maarten C. Mooij, Rob G. E. Timmermans, Wim Ubachs, Lorenz Willmann, Artem Zapara, and The NL-eEDM collaboration. Measuring the electric dipole moment of the electron in baf. *The European Physical Journal D*, 72(11):197, Nov 2018.

[2] S. Borri and G. Santambrogio. Laser spectroscopy of cold molecules. *Advances in Physics: X*, 1(3):368–386, 2016.

[3] Fritz-Haber-Institut der Max-Planck-Gesellschaft. Stark deceleration of molecular beams.

[4] N. J. Fitch, L. P. Parazzoli, and H. J. Lewandowski. Collisions between ultracold atoms and cold molecules in a dual electrostatic-magnetic trap. *Phys. Rev. A*, 101:032703, Mar 2020.

[5] B. Friedrich. A quasi-analytic model of a linear stark accelerator/decelerator for polar molecules. *The European Physical Journal D - Atomic, Molecular, Optical and Plasma Physics*, 31(2):313–336, Nov 2004.

[6] David J. Griffiths. *Introduction to Electrodynamics*. 2014.

[7] David J. Griffiths. *Introduction to Quantummechanics*. 2018.

[8] Koos Gubbels, Gerard Meijer, and Bretislav Friedrich. Analytic wave model of stark deceleration dynamics. *Phys. Rev. A*, 73:063406, Jun 2006.

[9] Van Swinderen Institute. Electron-edm.

[10] C. Meinema J. Nauta T.H. Nijbroek K. Jungmann H.L. Bethlem S. Hoekstra J.E. van den Berg, S.C. Mathavan. Traveling-wave deceleration of srf molecules. *Journal of Molecular Spectroscopy*, 300:22–25, Jun 2014.

[11] Mallikarjun Karra, Ketan Sharma, Bretislav Friedrich, Sabre Kais, and Dudley Herschbach. Prospects for quantum computing with an array of ultracold polar paramagnetic molecules. *The Journal of Chemical Physics*, 144(9):094301, 2016.

[12] Jeroen Maat. Calculations on the energy level structure and the effects of external fields in barium monofluoride, 2018.

[13] Jeroen Muller. Simulation of electric fields and molecular motion in a traveling-wave stark decelerator, 2017.

[14] James Stewart. *Calculus - Early Transcedentals*. 2015.

[15] Stephen T. Thornton and Jerry B. Marion. *Classical dynamics of particles and systems*. Brooks/Cole, Cengage Learning, 2008.

[16] Sebastiaan Y. T. van de Meerakker, Hendrick L. Bethlem, and Gerard Meijer. Taming molecular beams. *Nature Physics*, 4(8):595–602, Aug 2008.

[17] Sebastiaan Y. T. van de Meerakker, Hendrick L. Bethlem, Nicolas Vanhaecke, and Gerard Meijer. Manipulation and control of molecular beams. *Chemical Reviews*, 112(9):4828–4878, Sep 2012.

[18] J. E. van den Berg, S. H. Turkesteen, E. B. Prinsen, and S. Hoekstra. Deceleration and trapping of heavy diatomic molecules using a ring-decelerator. *The European Physical Journal D*, 66(9):235, Sep 2012.

[19] Eric W. Weisstein. Chebyshev polynomial of the first kind.

[20] Eric W. Weisstein. Modified bessel differential equation.

[21] Eric W. Weisstein. Modified bessel function of the first kind.

[22] Eric W. Weisstein. Modified bessel function of the second kind.

7 Appendix

7.1 Multivariable Taylor Expansion

When describing a complicated function in the neighbourhood of some point, it can be useful to expand said function into a Taylor series expansion. The Taylor series of a function expanded around the origin is named a Maclaurin series. The aim of this section is to build a compact and elegant operator to expand any scalar field into a series expansion.

A note about derivatives
The derivative operator is defined by its defining relation[14]:

$$d_x \equiv \frac{d}{dx},$$
$$d_x f(x) = \lim_{h\to 0} \frac{f(x+h/2) - f(x-h/2)}{h}.$$

Including a translation of the function $f(x) \to f(x+y)$ gives

$$d_x f(x+y) = \lim_{h\to 0} \frac{f(x+y+h/2) - f(x+y-h/2)}{h} = d_y f(x+y).$$

Which is to say that it does not matter whether x or y is varied when f is a function that depends only on the sum of both.

One-Dimensional Expansion
Suppose a function $g(t) : \mathbb{R} \mapsto \mathbb{R}$. The Maclaurin series of g can be written as[14]:

$$g(t) = \sum_{n=0}^{+\infty} \frac{g^{(n)}(0)}{n!} t^n = g(0) + g'(0)t + \frac{g''(0)}{2!}t^2 + ...,$$

where

$$g^{(n)}(t) \equiv \frac{d^n}{dt^n} g(t) = (d_t)^n g(t).$$

Now, suppose g is a translation of some other function f such that $g(t) = f(x+t)$. In that case

$$g(t) = \sum_{n=0}^{+\infty} \frac{g^{(n)}(0)}{n!} t^n = \sum_{n=0}^{+\infty} \frac{(d_t)^n g(0)}{n!} t^n = \sum_{n=0}^{+\infty} \frac{(d_x)^n f(x)}{n!} t^n = \left[\sum_{n=0}^{+\infty} \frac{(td_x)^n}{n!}\right] f(x).$$

Noting the definition of the exponent $e^x \equiv \sum_{n=0}^{+\infty} \frac{x^n}{n!}$, the expansion above can be cast into a compact form as

$$f(x+t) = e^{td_x} f(x). \tag{38}$$

Equation (38) describes the behaviour of f in the neighbourhood of x.

Multi-Dimensional Expansion
Take some scalar field $\phi(\vec{r}) : \mathbb{R}^n \mapsto \mathbb{R}$. This could for instance be the electric potential. Any point $\vec{r}$ in the neighbourhood of $\vec{r}_0$ can be written as a translation $\vec{r} = \vec{r}_0 + \hat{a}t$, where $\hat{a}$ is the unitvector pointing from $\vec{r}_0$ to $\vec{r}$ and t a parameter to denote the distance. Then

$$\phi(\vec{r}) = \phi(\vec{r}_0 + \hat{a}t) = \Phi(t),$$

which is a scalar function. Evaluation of the derivative of Φ will then be equivalent to computing the directional derivative[14] of ϕ in the $\hat{a}$ direction. That is,

$$d_t\Phi(t) = \hat{a} \cdot \vec{\nabla}\phi(\vec{r}).$$

Expanding $\Phi(t)$ into a Maclaurin series gives

$$\Phi(t) = \sum_{n=0}^{+\infty} \frac{\Phi^{(n)}(0)}{n!}t^n = \sum_{n=0}^{+\infty} \frac{(d_t)^n\Phi(0)}{n!}t^n = \sum_{n=0}^{+\infty} \frac{(\hat{a} \cdot \vec{\nabla})^n\phi(\vec{r}_0)}{n!}t^n = \left[\sum_{n=0}^{+\infty} \frac{(t\hat{a} \cdot \vec{\nabla})^n}{n!}\right]\phi(\vec{r}_0).$$

By absorbing t into $\hat{a}$ and once again noting the definition of the exponent, it is found that

$$\phi(\vec{r}_0 + \vec{a}) = e^{\vec{a}\cdot\vec{\nabla}}\phi(\vec{r}_0). \tag{39}$$

Equation (39) describes how to obtain the Taylor series of a scalar field around some point $\vec{r}_0$ in the $\hat{a}$ direction.

7.2 Degenerate Perturbation Theory

In describing the Stark shift of energy levels in an atom, perturbation theory starts to play a key role. What follows will be a derivation fitting the energy shift of a k-fold degenerate state. The derivations are inspired by the two-fold degeneracy described in[7].

Suppose a k-fold degenerate electronic state. That is,

$$H^{(0)}\psi_i^{(0)} = \mathcal{E}^{(0)}\psi_i^{(0)}; \qquad i = (1, ..., k), \tag{40}$$

$$\langle\psi_i^{(0)}|\psi_j^{(0)}\rangle = \delta_{ij}, \tag{41}$$

where the superscript (0) denotes the unperturbed case. So $H^{(0)}$ is the unperturbed Hamiltonian, $\psi_i^{(0)}$ the ith eigenstate and $\mathcal{E}^{(0)}$ the corresponding energy (independent of i). Any linear combination of eigenstates

$$\psi^{(0)} = \sum_{i=1}^{k} a_i\psi_i^{(0)}, \tag{42}$$

is still an eigenstate with the same energy $E^{(0)}$. Adding a perturbation $\lambda H'$ to the Hamiltonian gives

$$\begin{aligned} H &= H^{(0)} + \lambda H', \\ \mathcal{E} &= \mathcal{E}^{(0)} + \lambda\mathcal{E}^{(1)} + \lambda^2\mathcal{E}^{(2)} + ... , \\ \psi &= \psi^{(0)} + \lambda\psi^{(1)} + \lambda^2\psi^{(2)} + ... , \end{aligned}$$

where λ is just a temporary coefficient added to keep track of the perturbation order. Later, its value will be lifted to 1. Then becomes clear that the energy and the state are a sum of correction orders denoted by the superscript (i) in a power series. Putting these into the Schrödinger equation gives

$$H\psi = \mathcal{E}\psi,$$

$$(H^{(0)} + \lambda H')\sum_{n=1}^{+\infty}\lambda^n\psi^{(n)} = \sum_{n=1}^{+\infty}\sum_{m=1}^{+\infty}\lambda^{n+m}\mathcal{E}^{(m)}\psi^{(n)}.$$

Collecting like powers of λ gives

$$H^{(0)}\psi^{(0)} + \lambda(H'\psi^{(0)} + H^{(0)}\psi^{(1)}) + ... = \mathcal{E}^{(0)}\psi^{(0)} + \lambda(\mathcal{E}^{(1)}\psi^{(0)} + \mathcal{E}^{(0)}\psi^{(1)}) + ...$$

First-Order Correction
The first term left and right drops out from the unperturbed Schrödinger equation. Then, λ^1 says that

$$H'\psi^{(0)} + H^{(0)}\psi^{(1)} = \mathcal{E}^{(1)}\psi^{(0)} + \mathcal{E}^{(0)}\psi^{(1)}.$$

Taking an inner product with the ith unperturbed eigenstate:

$$\langle \psi_i^{(0)} | H' \psi^{(0)} \rangle + \langle \psi_i^{(0)} | H^{(0)} \psi^{(1)} \rangle = \mathcal{E}^{(1)} \langle \psi_i^{(0)} | \psi^{(0)} \rangle + \mathcal{E}^{(0)} \langle \psi_i^{(0)} | \psi^{(1)} \rangle .$$

Since $H^{(0)}$ is hermitian, it can be moved left in the second term left to cancel the second term right such that

$$\langle \psi_i^{(0)} | H' \psi^{(0)} \rangle + \mathcal{E}^{(1)} \langle \psi_i^{(0)} | \psi^{(0)} \rangle .$$

Substituting $\psi^{(0)}$ with its linear combination, equation (42), combined with the orthonormality condition (41) gives

$$\sum_{j=1}^{k} a_j \langle \psi_i^{(0)} | H' | \psi_j^{(0)} \rangle = a_i \mathcal{E}^{(1)},$$

or

$$\mathcal{E}_i^{(1)} = \sum_{j=1}^{k} \frac{a_j}{a_i} \langle \psi_i^{(0)} | H' | \psi_j^{(0)} \rangle . \tag{43}$$